

An observational and idealized numerical examination of low-level counter-rotating vortices in the rear flank of supercells

JERRY M. STRAKA

*School of Meteorology, University of Oklahoma
Norman, Oklahoma*

ERIK N. RASMUSSEN

*Rasmussen Systems
Mesa, Colorado*

ROBERT P. DAVIES-JONES

*National Severe Storms Laboratory
Norman, Oklahoma*

PAUL M. MARKOWSKI

*Department of Meteorology, Pennsylvania State University
University Park, Pennsylvania*

(Submitted 16 July 2007; in final form 31 December 2007)

ABSTRACT

Observations are reviewed that show that the dominant kinematic elements of the supercell rear flank are a downdraft trailing an adjacent updraft, a gust front, and counter-rotating vortices embedded in the gust front convergence zone. The associated vortex lines are shaped like arches. In an idealized simulation of the evolution of this flow structure, vortex rings are observed to form around a cool downdraft and in the adjacent periphery of the updraft. These rings are lofted in the rear portion of the updraft, and depressed in the downdraft. This resulting kinematic pattern strongly resembles the observations. Such a baroclinically-forced process is plausible in actual supercells, although it is uncertain whether it is ever sufficient for tornado formation, and to what extent the tilting of low-level quasi-streamwise vorticity plays a role.

1. Introduction

This paper presents an examination of a particular kinematic pattern that occurs in the low levels of the rear flank region of supercells and develops at scales smaller than the mesocyclone. The flow structure is found in most of the previously published dual-Doppler radar analyses, and precedes tornado formation in those storms that produced tornadoes. The low-level kinematic pattern consists of three associated features for an eastward moving storm: a cyclonic vorticity center, a gust front extending

from this vorticity center toward the east, and then approximately southward or southwestward and back westward into an anticyclonic vorticity center. The accompanying vortex lines are oriented upward in the positive vorticity region, turn quasi-horizontally toward the right (approximately southwestward) along the gust front, and then extend downward in the negative vorticity region. The quasi-horizontal segments are associated with a large forward-directed horizontal gradient of vertical velocity, between low-level updrafts above and to the east of the gust front and the trailing rear-flank downdraft to the west. This pattern is illustrated in Fig. 1. Though its occurrence generally has not been discussed in the literature, Markowski (2002) has reviewed instances in which counter-rotating vortices were documented.

Corresponding author address: Jerry M. Straka, School of Meteorology, University of Oklahoma, 120 David L. Boren Blvd., Ste. 5900, Norman, Oklahoma, 73072. E-mail: jstraka@ou.edu

This kinematic pattern is observed in both tornadic and non-tornadic supercells, so it is not an unambiguous predictor of tornadoes. We hypothesize that this signature reveals processes that perhaps are necessary but not sufficient for tornado formation.

We refer to the pre-tornadic cyclonic vorticity center as a tornado cyclone (Agee et al. 1976; Rasmussen and Straka 2007). Tornado occurrence associated with this kinematic pattern, or lack thereof, is partially a function of other factors such as low-level stability within the tornado cyclone (Leslie and Smith 1978; Markowski et al. 2002).

We note that the tornado cyclone described herein is *dynamically distinct* from the supercell mesocyclone. Historically, the mesocyclone has been understood to be partially the result of an arching vortex line process associated with an updraft acting upon westerly environmental shear, resulting in a mid-level anticyclonic vortex (mesoanticyclone) to the left, and an cyclone (mesocyclone) to the right, looking downshear (Davies-Jones 1984). In contrast, the process being described in this paper results in arches that are initially present in the low levels, and have an orientation generally opposite to that of the mid-level mesocyclone/mesoanticyclone pair. These arches cannot be explained readily by the drawing up of vortex lines associated with environmental shear. Hence, we seek a different explanation for the arching process that produces tornado cyclones versus the mesocyclone. Of course, as the tornado cyclone evolves, some of the vertical vorticity associated with the arching process may be advected upward through the storm and comprise part of the circulation identified as the mid-level mesocyclone.

The significance of the kinematic pattern is that it should be used to cull tornadogenesis hypotheses for their applicability to supercells. For example, the depressed vortex line hypothesis of Walko (1993) would not be consistent with the observed kinematic structure; sagging vortex lines, because they extend northward from anticyclonic to cyclonic vortices, more likely would be associated with sinking motion to the east and rising motion to the west. Hence, we might not expect to see a gust front, with the commonly observed southward-directed horizontal vorticity, if the Walko process were occurring. Nor would the so-called landspout hypothesis (Lee and Wilhelmson 1997) be consistent with the observed kinematic pattern; it

would be consistent with a single vortex, perhaps without an attendant gust front. Whatever hypotheses are suggested for supercell tornado cyclone formation, they should explain the occurrence of counter-rotating vortices connected by a gust front, with intense rising motion over/ahead of the gust front, and sinking (rear-flank downdraft) behind.

Historical examples of evidence of arching are presented in Section 2. In Section 3 a more detailed analysis of the rear-flank structure of a supercell observed in the Verification of the Origins of Rotation in Tornadoes Experiment (VORTEX, from Rasmussen et al. 1994) is described. In Section 4, we discuss hypotheses for the development of the arched vortex line pattern. In Section 5, we present a simple idealized numerical simulation of a downdraft/updraft pattern that produces the observed kinematic pattern. Finally, the work is concluded in Section 6.

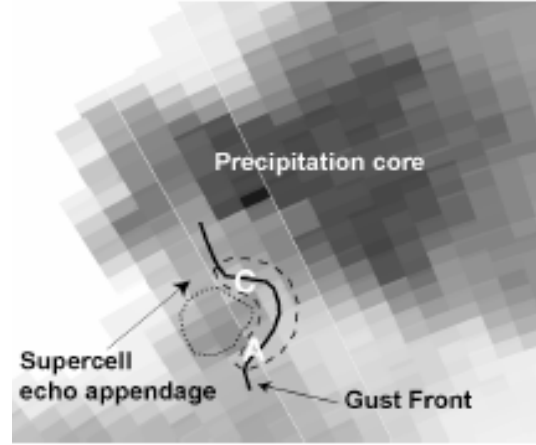


Figure 1. Schematic of the rear side of Dimmitt, TX supercell features. Shading represents radar reflectivity, with “C” denoting a cyclonic vorticity center, and “A” an anticyclonic vorticity center. The prominent low-level updrafts are enclosed by the broken line, with significant low-level downdrafts enclosed with a dotted line.

2. Historical evidence

In this section, we look at previously published supercell case studies that utilized dual-Doppler analysis. We include all cases with sufficient resolution for discerning the relevant kinematic structure, and we focus on analysis times depicting pre-tornadic flow. The exceptions are the Shamrock and Hill City (Table 1) storms that were non-tornadic. We note that Markowski (2002) provides a

comprehensive review of the research related to the supercell hook echo region. In this paper, the goal is to seek examples of a kinematic structure that previously was not identified clearly, possibly owing to an understandable focus on the tornado and tornado cyclone. The cases are summarized in Table 1, which contains references to figure numbers where analyses are reproduced and annotated herein.

Original figures from all of the previous studies have been reproduced and collated in Fig. 2. They have been modified to lessen the artifacts of digital scanning, and have been annotated to show the positions of the cyclonic vortex (marked "C") and anticyclonic vortex (marked "A"). Several authors marked gust front convergence zone locations in the original figures, and these have been retained with the original format. In some cases, we have added a thick black line to denote a region of large vertical velocity gradient or a probable gust front convergence zone location not annotated in the original. Finally, the panel label character has been changed from the original label to one corresponding to the fourth column in Table 1.

The kinematic pattern described in the Introduction is ubiquitous in these historical cases. All contain cyclonic vortices, regions of anticyclonic vorticity often found on the opposite side of a hook-like appendage, and evidence of gust fronts or zones of large forward-directed gradients of vertical velocity. As would be expected, the flow is typically strongest between the two vortices; hence, the strongest resolved flow typically is associated with the echo appendage that is also found between the two vortices (Brown and Knupp 1980). We note that the echo appendage itself often contains a local reflectivity maximum immediately behind the area of the vortices, perhaps implying a locally intense downdraft in that area as well.

In many of the original sources, analyses are shown for levels aloft. These verify the more complete kinematic picture of a downdraft trailing the surface gust front, locally intense low-level updrafts above the surface gust front, and an associated region of forward-directed gradient of vertical velocity in between. The anticyclonic vortex is typically the weaker one, and the gust front is generally more diffuse in its vicinity. Additional comments are made in later sections regarding this observation. Some notes on variations from the kinematic pattern are given in the "Comments" column of Table 1.

3. Observations of the pre-tornadic rear-flank region of the 2 June 1995 Dimmitt, TX storm

In the analyses of this and subsequent sections, vortex lines are used to gain an understanding of the structure of the flow and its evolution. Because vortex lines seldom are used in discussions of severe storms, a few explanatory comments may be helpful. The equation for the tendency of the vertical component of vorticity (e.g. Dutton 1976) is often used in supercell studies, but has two drawbacks: it has no means of describing the evolution of the horizontal components of vorticity that may be tilted into the vertical, and hence it is incapable of describing the very important role of baroclinic (solenoidal) generation that occurs mainly in the horizontal components. In most studies, the tendency equation produces the finding that tornadoes and tornado cyclones owe their existence to stretching of vertical vorticity, but this begs the question: what is the origin of vertical vorticity that subsequently was stretched? To describe adequately the flow evolution in the supercell rear flank, one would need to evaluate tendency equations for all three components of vorticity, but in practice this leads to complicated results that are very difficult to describe effectively.

In a barotropic, inviscid flow, vortex lines are frozen to the flow particles (Batchelor 1967). In a baroclinic flow (the supercell is arguably one of the most strongly baroclinic phenomena in the atmosphere) vortex lines do not move strictly with the flow. The constant generation of quasi-horizontal vorticity effectively causes a redistribution of vortex lines toward a more horizontal orientation. The barotropic part of flow evolution (original vortex lines simply moving with the flow) is still present. Furthermore, the lines of baroclinic vorticity that are generated in any small time interval after the initial time are subsequently carried with the flow (Davies-Jones 2006). Despite the baroclinic complication, vortex line analysis is very instructive in that it suggests plausible hypotheses for vorticity generation and redistribution. For example, if vortex lines appear in the flow as rings surrounding a downdraft, it could be surmised that the negative buoyancy and/or hydrometeor drag associated with the downdraft led to the generation of rings of vorticity.

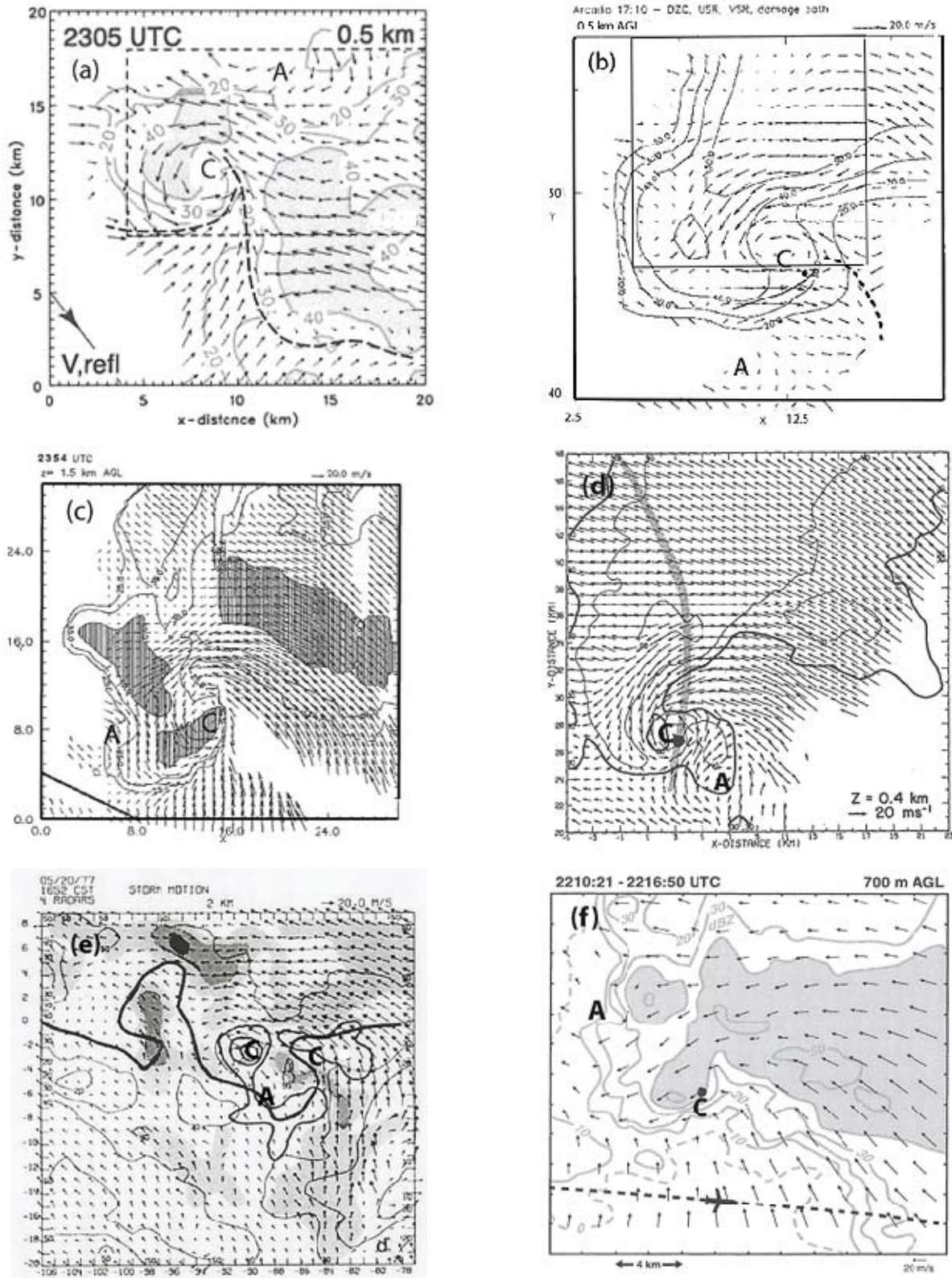


Figure 2. Analyses from the published literature (see Table 1). “C” marks the position of the cyclonic vortex, “A” the cyclonic vortex, and the heavy black line is the gust front convergence zone if not annotated by the original authors.

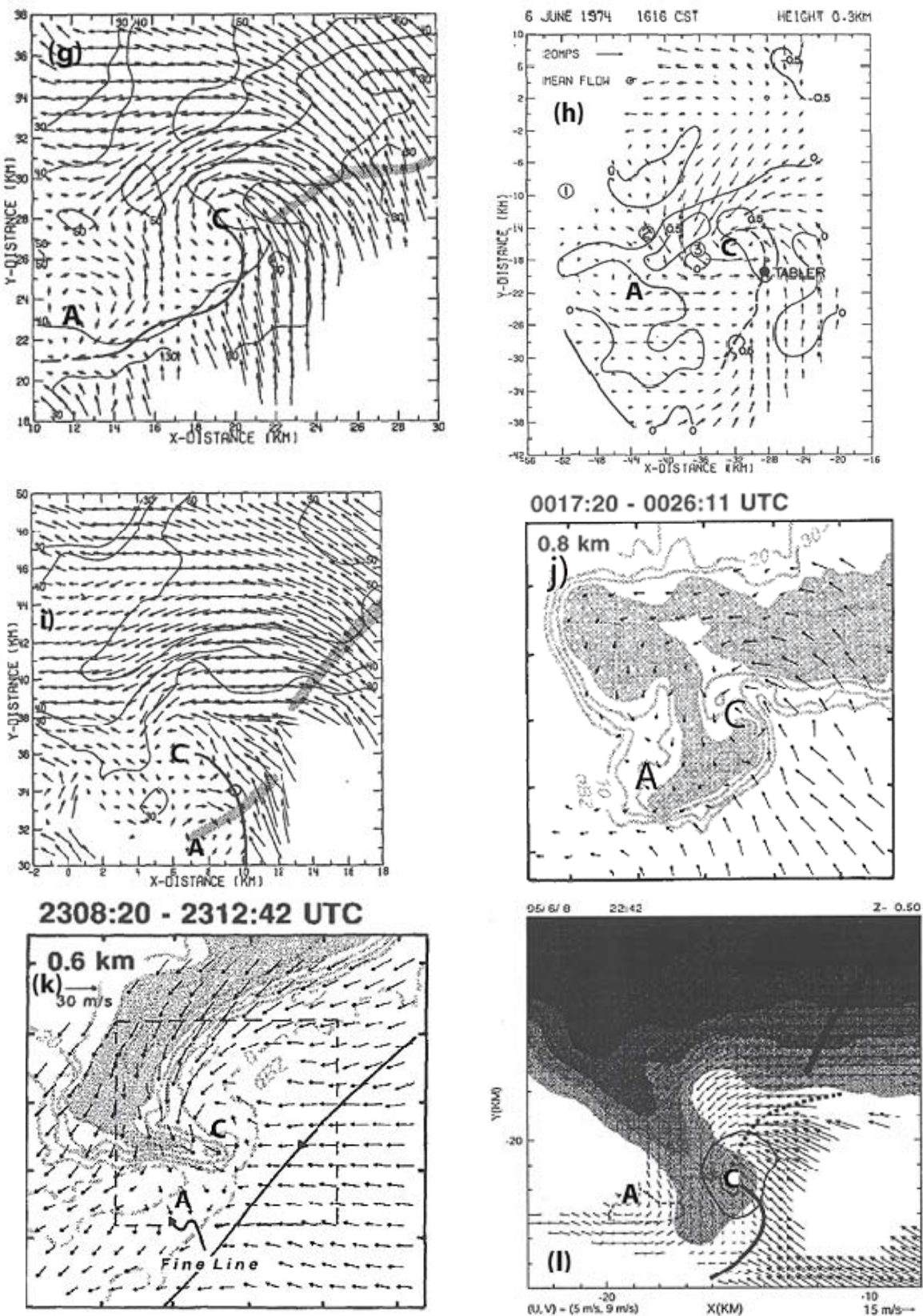


Figure 2 continued.

Table 1: Details of cases from the historical literature shown in Fig. 2.

Location/Date	Citation	Orig. figure num.	Panel in Fig. 2	Analysis elev. AGL	Comments
Newcastle, TX, 05/29/1994	Ziegler et al. (2001)	4e	a	500 m	Storm in northwesterly flow rotated about 90° from “typical” orientation.
Arcadia, OK, 05/17/1981	Dowell and Bluestein (1997)	5	b	500 m	
Shamrock, TX, 05/22/1995	Bluestein and Gaddy (2001)	9b	c	500 m	Non-tornadic supercell.
Del City, OK, 05/20/1977	Brandes (1984)	4	d	1300 m	Gust front hard to discern near “C”; anticyclonic vorticity extends along most of the back side of the hook echo.
Ft. Cobb, OK, 05/20/1977	Ray et al. (1981)	7	e	2000 m	Some of the original image has been cropped in Fig. 2.
San Angelo, TX, 05/31/1995	Wakimoto et al. (2004)	12a	f	700 m	Gust front diffuse near “A”.
Harrah, OK, 06/08/1974	Brandes (1978)	4	g	300 m	Gust front in original analysis extends from “C” to about 2 km south of “A”.
Tabler, OK, 05/08/1974	Brandes (1977)	4a	h	300 m	Original figure cropped. Gust front extends diffusely toward “A”.
Spencer-Luther, OK, 06/08/1974	Brandes (1978)	12	i	300 m	
Hill City, KS, 06/12/1995	Wakimoto and Cai (2000)	5d	j	800 m	Non-tornadic supercell. Anticyclonic vortex is weak and diffuse.
Garden City, KS, 05/16/1995	Wakimoto et al. (1998)	5e	k	600 m	“A” located in maximum anticyclonic shear; anticyclonic curvature extends further southwestward.
McLean, TX, 06/08/2005	Dowell and Bluestein, (2002a,b)	9a	l	700 m	Gust front position unknown to the south of “A” owing to lack of data.

Furthermore, vortex lines suggest dynamical connections between kinematic features that are easily overlooked using other analysis tools. The kinematic pattern being discussed in this paper is a good example: using vortex line analysis, a

cyclonic vortex, an updraft above a gust front with a trailing downdraft, and an anticyclonic vortex can be seen as *connected kinematic entities* (in this case, an interconnected region of large vorticity magnitude). Although the

vorticity dynamics cannot be quantified easily, the qualitative processes associated with the evolution of the flow are readily understood through the use of vortex lines (see Section 4).

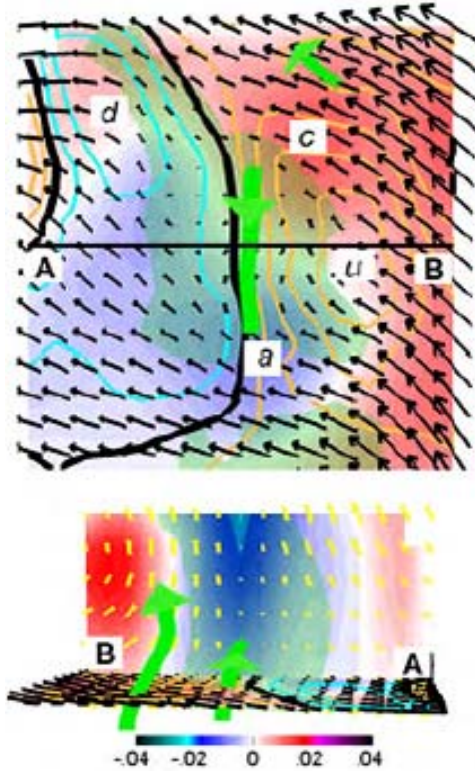


Figure 3. Analysis of the rear-flank region of the Dimmitt, TX supercell at 0050 UTC, 2 June 1995. Top panel is the horizontal plane at 700 m AGL. Color fills are vertical vorticity with scale as shown at bottom, the dominant cyclonic vortex marked "c", the dominant anticyclonic vortex marked "a", the updraft center "u", and the downdraft center "d". Horizontal wind vectors are spaced every 250 m with a grid-length vector denoting 10 m s^{-1} . Contours are vertical motion w at 1 m s^{-1} interval, cyan for negative, orange for positive, and zero being heavy black. The green arrows are three-dimensional vortex lines. The line A-B refers to the perspective view in the bottom panel, looking from 350° azimuth. The same two vortex lines are shown. Velocity in the A-B plane is shown with yellow vectors, 20 m s^{-1} per grid length. Vertical grid spacing is 500 m. Color shading is the northward component of horizontal vorticity with the same color scale as the top panel. Green transparency in both panels denotes ELDORA reflectivity $> 30 \text{ dBZ}$.

Dual-Doppler radar analysis (see Appendix for details) has been performed for a tornadic supercell that occurred near Dimmitt, TX on 2 June 1995 during VORTEX. The general pattern of cyclonic vortex, gust front, and anticyclonic vortex shown in the previous examples also was present in this case at a time about 9 min prior to tornado formation (Fig. 3). Two vortex lines are shown, representing two general families of lines. In the southwestern part of the cyclonic vortex, the vortex lines arch upward, then southward, and then return downward in a region of anticyclonic vorticity to the south. The southward-extending vortex line is in a region of large negative (southward) horizontal vorticity, between the updraft above the gust front and the trailing downdraft. Note that the vortex pair is embedded in the periphery of a column of precipitation that has radar reflectivity $> 30 \text{ dBZ}$. This feature has been described as a descending reflectivity core (DRC, after Rasmussen et al. 2006) and ongoing research shows that it is a relatively common feature in tornadic supercells (Kennedy et al. 2007). Indeed, it is this somewhat isolated column of precipitation, pendant from the echo overhang aloft, that motivated this exploration of the effects of a local precipitation-induced downdraft. A second vortex line is shown, typical of the vortex lines in the northeast half of the cyclonic vortex. It extends almost straight upward from near the ground. One possible explanation for this family of lines is the tilting of inflow air rich in streamwise vorticity. In fact, the near-ground vortex lines in the inflow region of the storm are oriented northwestward, and are strongly streamwise. Insufficient Doppler radar data exist to evaluate the temporal evolution of the arching vortex line pattern at other times prior to the tornado.

4. Hypothesis for the arching vortex line phenomenon

In order to establish the applicability of the hypothesis explored here, we briefly review important information concerning supercell tornadoes. The majority of tornadoes and essentially all violent ones form in association with supercells. They have been observed to develop in association with low-level mesocyclones, or circulations on the order of 2 to 10 km in diameter that often reach far upwards in the supercell storms, and last for an order of one to several hours. Supercell-type tornadoes form on the storm's rear right flank, which often is the southwest flank in near proximity to the rear-

flank downdraft. Circulations, sometimes called tornado cyclones, from which these tornadoes come, are the focus of this research.

Tornado cyclones may have a different origin than the mesocyclone as shown herein. Tornado cyclones and tornadoes generally form with classic supercells, but also can occur with low-precipitation and high precipitation supercells, though with less frequency (Rasmussen and Straka 1998). An optimal amount of precipitation associated with the hook echo seems to be the reason for classic supercells to be such prolific producers of tornadoes. Supercell storms that produce significant tornadoes form in environments with vertical wind shear that have large storm-relative helicity (Davies-Jones 1984) associated with significant turning of the storm relative wind clockwise with height in the lowest 3 km, and especially in the lowest 1 km of the atmosphere.

One hypothesis for vortex line arching and tornado cyclone genesis is the following (Davies-Jones 1996, 2000 hinted at this process): First, precipitation is needed. It has been found from numerical simulations that tornadoes do not form in simulations with precipitation processes turned off. As dry air flows through the precipitation at the rear of the storm, a downdraft forms, with stronger downward motion at its center (Fig. 4b). This downdraft is associated with a toroidal circulation and the vortex rings begin to advect downward owing to being associated with downdraft air. The vortex rings are elongated downstream because of the horizontal wind. They then become tilted by the updraft as they enter the zone separating the rear-flank downdraft and updraft boundary. As the toroidal circulation approaches the ground, the leading edge is advected upward in the low-level updraft, leading to arch-shaped vortex lines with positive vorticity to the left (north) and negative vorticity to the right (south; Fig. 3). Tilting of baroclinic vorticity as described above is thus hypothesized to be the reason for the tornado cyclone itself.

It seems plausible that the rear-to-front advective flow posited in the Davies-Jones (2000) hypothesis perhaps is not required. As shown in the next section, the arching process can proceed without ambient rear-to-front flow. Under certain idealized conditions, the generation of horizontal vorticity associated with a localized downdraft can lead to an overall advection of vortex rings

into a position beneath the updraft (Fig. 4c), where they subsequently can be drawn up into arches. One can visualize that simple spreading of the downdraft as it approaches the surface could also place vortex rings into the region below an adjacent updraft.

Note the significant difference from the two examples that demonstrate the arching process discussed at length in this paper (Fig. 4b, c). In one case we show that rear-to-front flow pushes the leading edge of the vortex rings forward. The leading edges of the rings are tugged upward as they are pushed into the updraft (Fig. 4b), producing the observed arching pattern and subsequently the counter-rotating vortex pattern. The upwind edges of the vortex rings are constantly regenerated and appear stationary in a storm-relative sense as long as there is a baroclinic generation mechanism such as cooling or a combination of loading and drag. In another example we show that spreading of vortex rings occurs as the rings approach the ground. Subsequently, in the lower part of the atmosphere, the rings also are tugged upward producing the observed arching pattern (Fig. 4c). Either case (b) or case (c) is plausible, and it is likely that a combination of these actions is occurring.

The vortex lines in Fig. 4a follow the experiments designed by Walko (1993) in his simulation of a tornadic supercell storm. This vortex line configuration seems relatively implausible for the reasons discussed in the Introduction.

5. Numerical simulation

The foregoing hypothesis and observations have motivated us to perform an idealized numerical experiment to understand the prevalent kinematic pattern that precedes tornado formation in the rear flank region of supercells. Hence, one must consider the effects of vertical drafts in tilting storm-generated baroclinic horizontal vorticity. The preponderance of historical observations shows that the vortex couplet occurs in close proximity to the rear-flank gust front. It is the horizontal vorticity associated with shear between the main storm updraft and the trailing rear-flank downdraft that perhaps is most likely to be reoriented into a vertical orientation in this region of a supercell. We hypothesize that vortex lines, initially oriented quasi-horizontally in this region, can be reoriented simply by the updraft and downdraft

to produce the observed pattern of vortices and gust front. Further, we hypothesize that this process can occur even in the explicit absence of vertical shear of the ambient flow. For the sake of clarity in interpreting numerical simulation

results, we sought to model the simplest mechanism consistent with the supercell observations above.

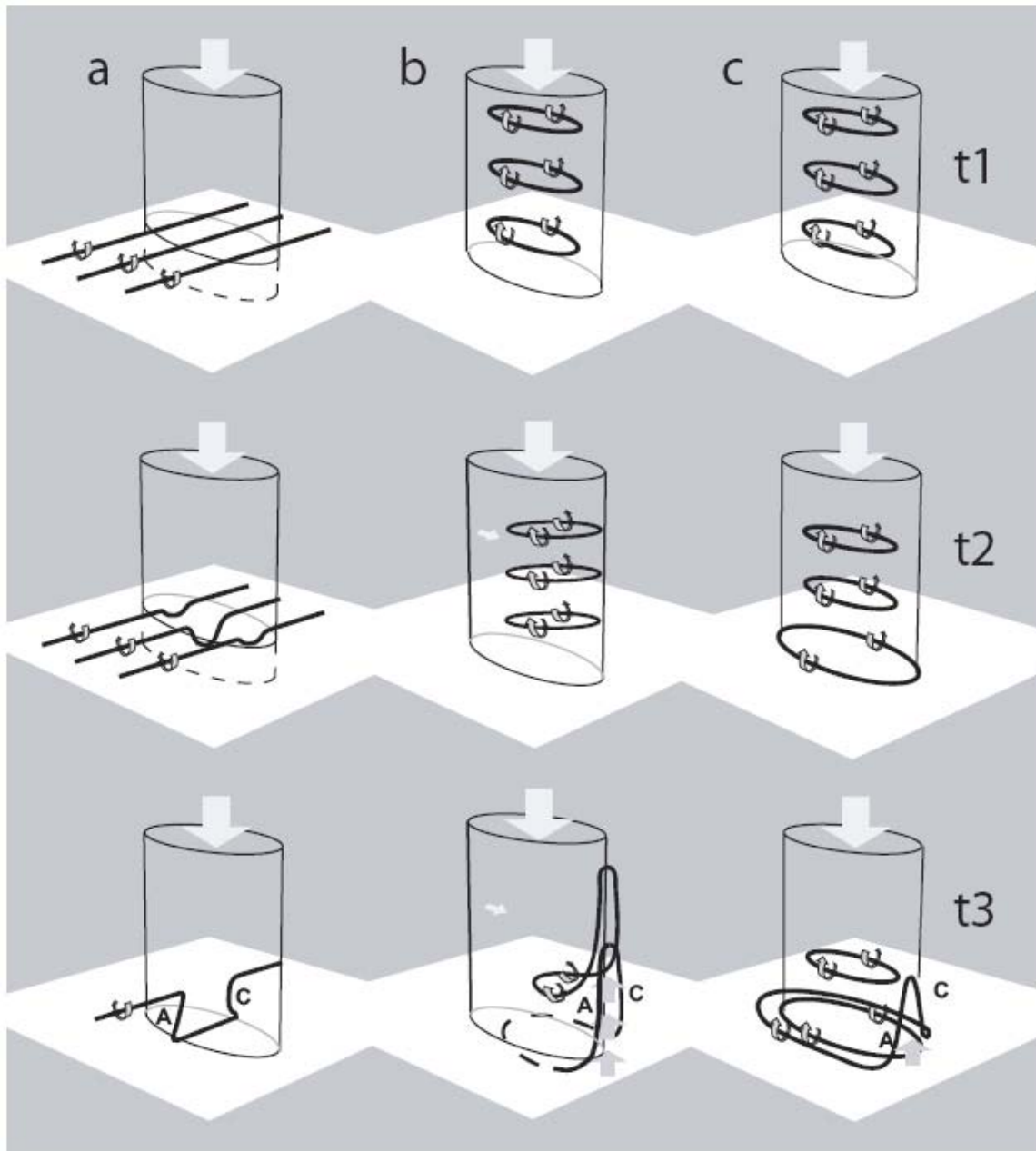


Figure 4. Schematic of Walko's (1993) hypothesis (a) and two versions of the arching hypothesis (b,c). The letters "A" ("C") denote cyclonic (anticyclonic), solid lines are vortex lines, and t1, t2 and t3 are increasing relative time increments.

a. Initial conditions for the model

The cloud model used in this study is a compressible, non-hydrostatic model that is described in Straka and Anderson (1993), and Straka and Mansell (2005). The grid consisted of 82x82x82 grid points with resolution of 500 m horizontal and 250 m vertical. A damping layer was specified above 15 km. The model was initialized with a bubble 10.8 km in diameter, 2 km deep, centered at 1900 m AGL in the middle of the plane. The thermal perturbation was 2 K, following somewhat the initial conditions for the updraft by Klemp and Wilhelmson (1978). The ambient thermodynamic profile is taken from the model sounding of Weisman and Klemp (1982) with a boundary layer mixing ratio of $1.4 \times 10^{-2} \text{ kg kg}^{-1}$. At the initial time, a rain source of $5 \times 10^{-6} \text{ kg kg}^{-1} \text{ s}^{-1}$ is present at 5 km AGL, with a radius of 3 km and a vertical extent of 2 km. The rain source is located along the centerline of the domain above the rear periphery of the warm bubble initially, loading the subsequently developing updraft and evaporatively cooling the air. This position was chosen to approximate the observed DRC (Rasmussen et al. 2006), which is a column of precipitation that descends in the rear periphery of a supercell updraft, with the outflow of the downdraft spreading out horizontally at the ground (this has an implicit effect of producing some shear in and atop the outflow). The rain descends with time, while the source remains fixed in position. During the simulation, the updraft is allowed to evolve naturally. Cloud water is allowed in the simulation, but rain is prohibited from forming in the updraft. This allows the updraft to persist in the absence of shear that normally is required to remove the precipitation. Thus, the essence of this experiment is to investigate how flow evolves when a downdraft forms in the rear side of an updraft in the absence of ambient shear. This experiment has been repeated with ambient low-level westerly shear, and the results are qualitatively the same. The experiments with shear represent the next level of complexity, and will be reported in a subsequent paper.

b. Results

The evolution of this simple idealized flow is depicted at four-minute intervals in Fig. 5. In the early stages (20, 24 min), the rain (blue transparency) descends to the rear of the updraft maximum, reaching 1500 m AGL at around

24 min. Associated with the arrival of the rain, the downdraft intensifies markedly at that level. The perspective view shows that southward horizontal vorticity (blue and green shades in vertical planes) intensifies and develops downward with the descent of the rain. Quasi-horizontal rings of vorticity (not shown) encircle the downdraft, passing through the deep column of southward horizontal vorticity. As early as 18 min, and clearly visible at 20 and 24 min, a couplet of vertical vorticity is present in the 1500 m plane (pink [positive] shades to north; blue [negative] shades to south in horizontal plane). Vortex lines (not shown) arch upward from the cyclonic element and descend through the anticyclonic one. However, these lines are part of small-scale loops that encircle the minor weakness in the updraft enclosed by the 2 m s^{-1} contour.

Figure 5 (following pages). Simulation of the arching process. Left-hand panels are horizontal plane data at $z=1500 \text{ m}$, except for the heavy green line which is a three-dimensional vortex line cutting the 1500 m plane near the maximum in vertical vorticity. The vortex line is drawn as a narrow broken green line where hidden below the horizontal plane. Vertical vorticity is shaded red and blue according to the scale shown. Horizontal wind vectors are black with 10 m s^{-1} magnitude equivalent to one grid length. Color contours are w at 1 m s^{-1} intervals, heavy black denoting zero, magenta positive, and cyan negative (labeled in ambiguous areas). Transparent green shading denotes rainwater content larger than 0.01 g kg^{-1} . Right-hand panels are perspective views from 350° azimuth as shown in the top left-hand panel with the A-B vertical plane line and perspective arrow. Vorticity is the northward-directed horizontal component colored with the same scale as vertical vorticity (generally larger than vertical vorticity). Velocities in the bisecting plane (yellow vectors) are scaled by 20 m s^{-1} per one grid length. The heavy green field line is the same vortex line as in the left-hand panels

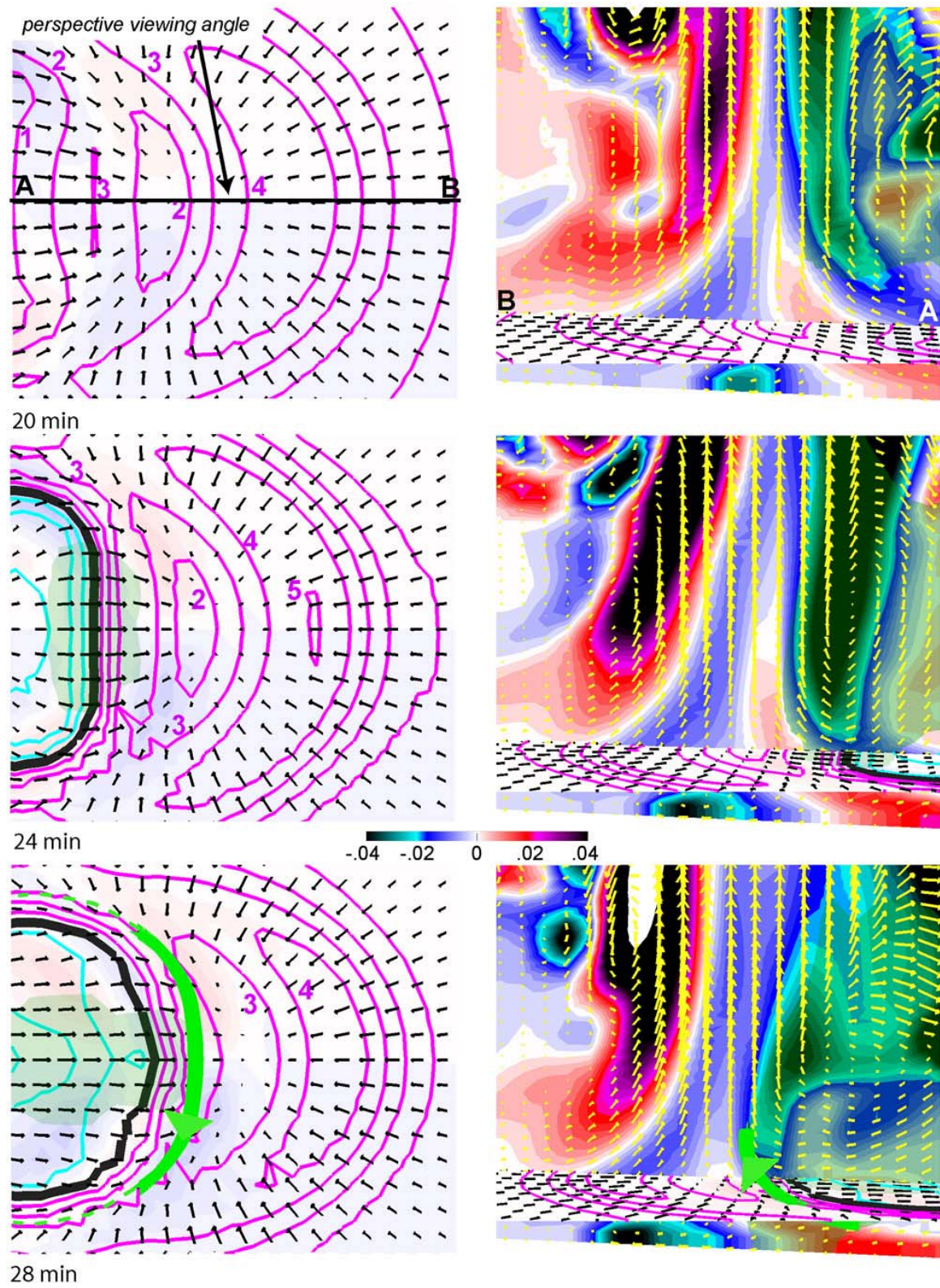


Figure 5.

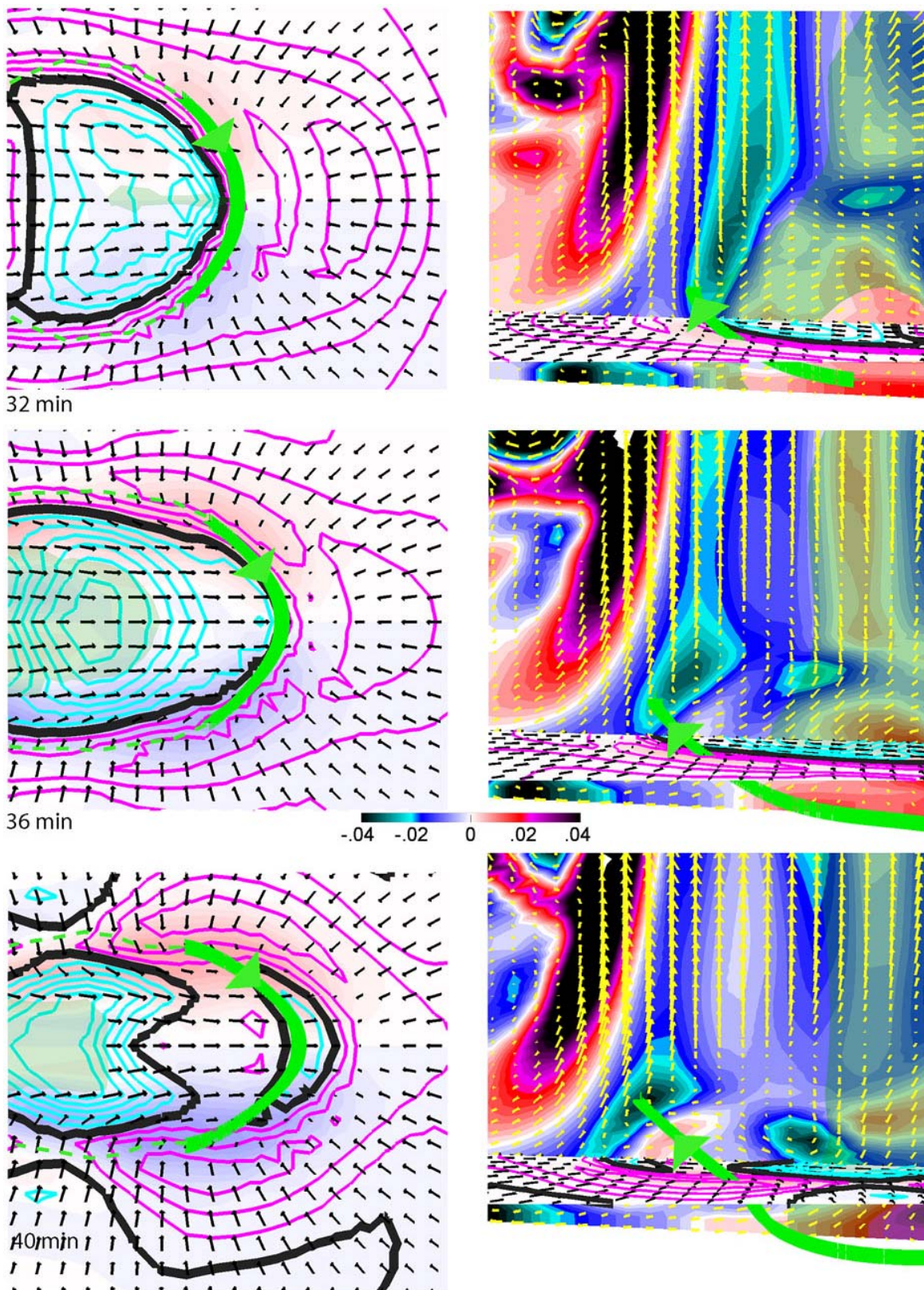


Figure 5 continued.

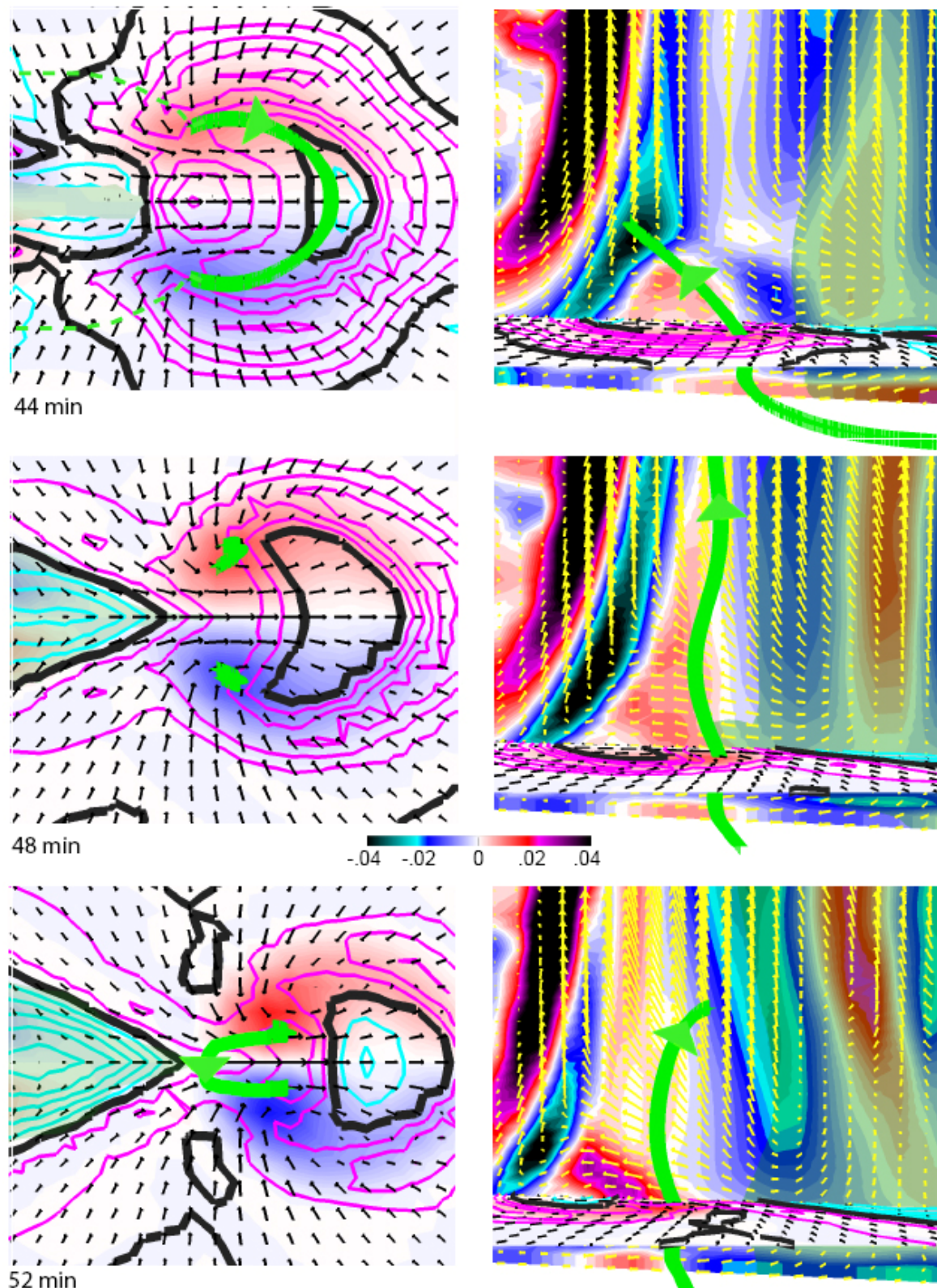


Figure 5 continued.

The kinematic structure described in the preceding sections (vortex line arching pattern) begins to develop around 28 min. At that time, we illustrate the vortex line arching process using a single line (bright green) that passes approximately through the largest magnitude vertical vorticity at 1500 m AGL. It should be understood that this line is representative of vortex lines throughout the vorticity couplet. The vortex line extends quasi-horizontally rearward, encircling the downdraft, but is tugged up slightly at the leading edge where it is located in updraft. In fact, horizontal vorticity generally is negative throughout the region from the axis of the updraft to the axis of the downdraft. It is also apparent at 28 min that horizontal vorticity (as well as rainwater) is being advected forward toward the updraft in lower levels owing to the larger-scale overall circulation associated with the negative vorticity region. Thus the net effect of the forward and upward advection of vortex lines at 28 min in this simulation is the development of counter-rotating vortices with increasing rear-to-front flow between them (most apparent in the horizontal 1500 m plane). The horizontal acceleration is associated with the development of an arc shape to the gust front convergence zone.

It is tempting to explain the arching pattern as gust front vorticity that has been tugged upward in the low-level updraft. But this simplification is inadequate: the gust front and the localized intense horizontal vorticity associated with it can be seen in the perspective views (below the 1500 m plane) as having advanced a few kilometers beyond the arched vortex line region. This simplified explanation becomes more adequate if one considers the "gust front" to be a sloping region of intense horizontal vorticity extending upward and rearward toward the precipitation column.

The structure at 28 min has important similarities to the Dimmitt example shown previously: the arched vortex line has a similar shape, and the gust front and updraft have attained a slightly arcing shape. Note that evolution occurs very quickly during this part of the simulation, as it did in the Dimmitt storm, which produced a tornado 9 min after the time of the analysis shown. By the time of the tornado near Dimmitt, the gust front had surged roughly 10 km south and east, ahead of the developing tornado.

Features of the simulation apparent by 28–32 min, that are similar to observed supercell structures, include the following: horseshoe-shaped updraft (e.g., Brandes 1978; Klemp and Rotunno 1983), surging gust front, counter-rotating vortices (Markowski 2002 and Sec. 1 herein), and the cyclonic vortex. In the region of large gradients of vertical velocity, the vortex contains both upward and downward motion, but is centered in positive vertical velocity (Brandes 1978). Note that all of these features, including the shape of the updraft, are a consequence of the baroclinically-driven vorticity dynamics.

By 40 min, the vortex line has become more erect (increasing vertical vorticity) as the forward side continues to be advected upward, and the rear portion settles toward the lower boundary. The length of the vortex line, which is contained in a vortex tube, is increasing owing to longitudinal stretching of vortex tubes, which increases vorticity. The resultant increase in circulation about this collection of vortex lines leads to an interesting local feature: downward motion to its immediate rear causes a downdraft to appear immediately behind the gust front at 1500 m.

This is strongly reminiscent of field observations near developing tornadoes, with striking downward motion immediately behind the gust front (the simulated downward motion is almost certainly weaker than the observed). The authors and other storm chasers sometimes have described the motion of dissipating cloud fragments at that location as resembling a waterfall. Developing circulation about the horizontal in the gust front convergence zone is thus an alternative hypothesis for the intense sinking often observed immediately behind the gust front.

During the period of 44 to 52 minutes, the development of vertically oriented, intense (vertical vorticity $\sim 2 \times 10^{-2} \text{ s}^{-1}$; similar to observed tornado cyclones) counter-rotating vortices is completed; a period of about 30 min. At 44 min, the vortex line extending through the vertical vorticity maxima at 1500 m continues to be arch-shaped, but has become nearly vertical in lower levels. By 48 minutes, the arch has been advected out of the top of the domain shown, resulting in deep vertically oriented vortices. Consistent with observations, the vortices lag well behind the surging low-level gust front.

Furthermore they form without ambient wind shear and the presence of a preexisting source for vorticity except the horizontal vortex lines around the updraft and downdraft.

Finally, we note that the vortices do not become as intense in the lowest levels as they would if we had included friction. However, the goal of this experiment was to study a simple process of tilting storm-generated vorticity and the associated arched vortex line pattern that is typically observed.

To add credence to the foregoing interpretation of the simulated processes, we have opted for a very simple approach. We computed the forcing terms of the vorticity tendency equation for three points found along the incipient arch at 28 min, and a mature arch at 36 min. Computations of forcing terms (tilting, stretching, advection generation of all three vorticity components) at these points were carried out 2 min prior to the nominal analysis times, because we sought to learn how the arch came to exist at those points, instead of how it was evolving at the time it was found at those points.

Considering the highest point of the arch, which occurs in the east-west vertical plane in the center of the domain, the forcing is completely dominated by vertical advection of the southward-directed vorticity. In other words, the arch is being lofted at that point by the strong updraft, consistent with an intuitive interpretation based on the figures shown earlier.

At the point where the arch emerges from the 1500 m elevation horizontal plane, in the incipient cyclonic vortex, the total generation rate of vertical vorticity is an order of magnitude larger than the generation rate of the horizontal vorticity components. Tilting is the largest forcing term by an order of magnitude. This finding answers the question posed above: in this idealized simulation, the vertical vorticity first arises through the tilting of horizontal vorticity, again consistent with the intuitive interpretation that a horizontal vortex ring is being reoriented. At a point intermediate to these two, the magnitude of vorticity generation is similar through all processes and orientations, but it is interesting to note that the tilting terms are giving rise to vorticity that is increasingly upward and toward the southeast; i.e., along the arch.

Later (36 min arch locations), consistent with historical observational studies, the generation of vorticity is largely in the vertical component and is largely due to stretching as the arch exists in a velocity field characterized by large increases of vertical velocity with height. Only near the apex of the arch did the vertical advection of southward-directed vorticity continued to dominate.

6. Conclusions

In surveying the historical literature, a consistent kinematic pattern is observed prior to supercell tornadogenesis. Looking along the storm motion vector, this pattern at the rear flank of the storm consists of a cyclonic vortex to the left, an anticyclonic vortex to the right, with the vortices connected by a convergence zone that is typical of a thunderstorm gust front. Additionally, the historical studies depict (or imply) the well-known, intense, low-level updraft above and ahead of the gust front, and a rear-flank downdraft trailing the gust front. Unfortunately, it is sometimes the case that radar observations are very limited in the vicinity of the anticyclonic vorticity center because of low reflectivity.

In a number of supercells observed by dual or multiple Doppler, including the 2 June 1995 Dimmitt, TX tornadic supercell, the vortex lines rose in the cyclonic vortex, turned south quasi-horizontally parallel to the gust front, and then descended in the anticyclonic vortex. Hence, we suggest that hypotheses that are put forth to explain events prior to supercell formation ought to include an explanation of near ground rear-flank vortex line arching.

A simple, idealized, numerical simulation of only the grossest elements of the supercell rear flank, a downdraft partially embedded in the rear of an adjacent updraft, produces vortex line arching consistent with the observations. Vortex rings form around a simulated cool downdraft and in the adjacent periphery of the simulated updraft. These rings are lofted in the rear portion of the updraft, and depressed in the downdraft. Such a baroclinically-forced process is plausible in actual supercells, although it is very uncertain whether it is ever sufficient for tornado formation, and to what extent the tilting of low-level barotropic (~streamwise) vorticity plays a role. Other theoretical and numerical studies have demonstrated somewhat similar, simple mechanisms for the reorientation of baroclinic

vorticity by an updraft (Davies-Jones 1996; Weisman and Davis 1998; and Shapiro and Kanak 2002).

In our experiment, there is no mechanism that would favor one vortex over the other for tornado formation. But the observations clearly show that the cyclonic vortex generally is the dominant one, with the anticyclonic vortex and the nearby gust front being weaker and more diffuse. In nature, it is plausible that the cyclonic member experiences greater stretching owing to proximity to the intense low-level updraft, whereas the anticyclone is typically farther removed from the updraft (Davies-Jones et al. 2001). Likewise, it is possible that the inflow being tilted at the gust front contains streamwise vorticity that would contribute to the circulation of the cyclonic member (e.g. Dowell and Bluestein 2002b). The sensitivity of the rear-flank evolution to these factors is being explored in another, somewhat more complicated, series of simulations.

We would like to emphasize what this paper does not claim to do. We cannot claim that our idealized simulation explains the genesis process of counter-rotating vortices in the supercell-like storms in their rear flank. That these vortices exist is amply demonstrated by the historical data. That a fluid such as the atmosphere, with certain highly idealized initial conditions, can produce a similar structure has also been demonstrated herein. However, we cannot demonstrate through the evidence or the simulation that the baroclinic process, associated with the special buoyancy distribution in an updraft, is the mechanism that produces the observed kinematic structure. Presently, the mechanism must be regarded as a hypothesis that has plausible fluid dynamics and is relatively consistent with the observations. Refuting the hypothesis will entail much careful analysis of detailed four-dimensional velocity data from high-resolution field observations or cloud models with validated microphysical treatments. Further, by posing the hypothesis, we hope to motivate additional numerical experiments and focused field observations.

ACKNOWLEDGMENTS

We are grateful to Dr. Bob Conzemius for his review and Dr. Chuck Doswell for reading the paper earlier. This paper was supported by NSF Grant ATM 0340693.

APPENDIX

During the pre-tornadic phase of the Dimmitt, Texas supercell of 2 June 1995, only limited data were collected that are suitable for dual-Doppler analyses. The airborne Doppler data from one aircraft did not extend far enough southward to capture the low-level mesocyclone, and data were missing from the “fore” scan of the ELDORA airborne radar (Hildebrand et al. 1994). Hence, for this analysis, data are combined from the prototype DOW (Doppler on Wheels, from Wurman et al. 1997) and the “aft” scan of the first fly-by of the ELDORA radar.

The dual-Doppler data have been analyzed objectively using a one-pass Barnes approach (Barnes 1964), with a Gaussian weighting function preserving 75% response at ~ 1500 m wavelength (the worst sampling by the two radars was in the ELDORA data in the along-track direction, with 1500 m comprising roughly four along-track samples). The ELDORA data were collected from an altitude of about 700 m AGL, and all data were advected using an overall storm motion of 250° at 14 m s^{-1} to a common analysis time of 0049:15 UTC. The horizontal grid spacing was 350 m with the horizontal domain including the DRC and nearby areas. The vertical grid spacing was 500 m, with the first grid level at 200 m AGL. Data were analyzed only in the lowest ~ 3 km because of shallow coverage from the DOW. Further, scatterer vertical motion was assumed not to contribute to Doppler velocity owing to the small elevation angles of the radar rays (generally $< 10^\circ$). Vertical velocity was computed by integrating the anelastic continuity equation upward from a boundary condition of $w=0$ at $z=0$ m AGL. The data from ELDORA were collected between 0049:42 and 0050:55 UTC, while those from the DOW were collected between 0047:16 and 0049:15 UTC.

It should be noted that this dual-Doppler analysis combining data from airborne and surface mobile platforms has not been tuned to capture fine scale details, but instead only the bulk features of the flow are of interest here. The analysis method is suitable for confirming the kinematic features associated with vortex line arching described in Sec. 1.

REFERENCES

Agee, E. M., J. T. Snow, and P. R. Clare, 1976: Multiple vortex features in a tornado cyclone and the occurrence of tornado families. *Mon. Wea. Rev.*, **104**, 552-563.

Barnes, S. L., 1964: A technique for maximizing details in numerical weather map analysis. *J. Appl. Meteor.*, **3**, 396-409.

Batchelor, E. K., 1967: *An Introduction to Fluid Dynamics*. Cambridge Press, 615 pp.

Bluestein, H. B. and S. G. Gaddy, 2001: Airborne pseudo-dual-Doppler analysis of a rear-inflow jet and deep convergence zone within a supercell. *Mon. Wea. Rev.*, **129**, 2270-2289.

Brandes, E. A., 1977: Gust front evolution and tornadogenesis as viewed by Doppler radar. *Mon. Wea. Rev.*, **19**, 113-120.

—, 1978: Mesocyclone evolution and tornadogenesis: Some observations. *Mon. Wea. Rev.*, **105**, 995-1011.

—, 1984: Vertical vorticity generation and mesocyclone sustenance in tornadic thunderstorms: The observational evidence. *Mon. Wea. Rev.*, **112**, 2253-2269.

Brown, J. M., and K. Knupp, 1980: The Iowa cyclonic-anticyclonic tornado pair and its parent thunderstorm. *Mon. Wea. Rev.*, **108**, 1626-1646.

Davies-Jones, R. P., 1984: Streamwise vorticity: The origin of updraft rotation in supercell storms. *J. Atmos. Sci.*, **41**, 2991-3006.

—, 1996: Formulas for barotropic and baroclinic components of vorticity with applications to vortex formation near the ground. *Preprints, 7th Conf. on Mesoscale Processes*, Reading, England, United Kingdom, Amer. Meteor. Soc., 14-16.

—, 2000: Tornado. McGraw-Hill. [Available online at: <http://www.accessscience.com/content.aspx?id=701400>]. doi: 10.1036/1097-8542.701400.

—, 2006: Integrals of the vorticity equation. Part I: General three- and two-dimensional flows. *J. Atmos. Sci.*, **63**, 598-610.

—, R. J. Trapp, and H. B. Bluestein, 2001: Tornadoes and Tornadic Storms. *Severe Convective Storms, Meteor. Monograph*, **28**, Amer. Meteor. Soc., Boston, MA, 126-221.

Dowell, D. C. and H. B. Bluestein, 1997: The Arcadia, Oklahoma, storm of 17 May 1981: Analysis of a supercell during tornadogenesis. *Mon. Wea. Rev.*, **125**, 2562-2582.

—, 2002a: The 8 June 1995 McLean, Texas, storm. Part II: Cyclic tornado formation, maintenance, and dissipation. *Mon. Wea. Rev.*, **130**, 2649-2670.

—, 2002b: The 8 June 1995 McLean, Texas, storm. Part I: Observations of cyclic tornadogenesis. *Mon. Wea. Rev.*, **130**, 2626-2648.

Dutton, J. A., 1976: *The Ceaseless Wind*. McGraw-Hill, 579 pp.

Hildebrand, P. H., C. A. Wallther, C. L. Frush, J. Testud, and F. Baudin, 1994: The ELDORA/ASTRIA airborne Doppler weather radar: Goals, design, and first field tests. *Proc. IEEE*, **82**, 1873-1890.

Kennedy, A., J. M. Straka, and E. N. Rasmussen, 2007: A statistical study of the association of DRCs with supercells and tornadoes. *Wea. Forecasting*, in press.

Klemp, J. B., and R. B. Wilhelmson, 1978: Simulations of right- and left-moving storms produced through storm splitting. *J. Atmos. Sci.*, **35**, 1097-1110.

—, and R. Rotunno, 1983: Study of the tornadic region within a supercell thunderstorm. *J. Atmos. Sci.*, **40**, 359-377.

Lee, B. D., and R. B. Wilhelmson, 1997: The numerical simulation of nonsupercell tornadogenesis. Part II: Evolution of a family of tornadoes along a weak outflow. *J. Atmos. Sci.*, **54**, 2387-2415.

Leslie, L. M., and R. K. Smith, 1978: The effect of vertical stability on tornadogenesis. *J. Atmos. Sci.*, **35**, 1281-1288.

Markowski, P. M., 2002: Hook echoes and rear flank downdrafts: A review. *Mon. Wea. Rev.*, **130**, 852-876.

—, J. M. Straka, and E. N. Rasmussen, 2002: Direct surface thermodynamic observations within the rear-flank downdrafts of nontornadic and tornadic supercells. *Mon. Wea. Rev.*, **130**, 1692-1721.

Rasmussen, E. N., and J. M. Straka, 1998: Variations in supercell morphology. Part I: Hypotheses and observations. *Mon. Wea. Rev.*, **126**, 2406-2421.

—, —, 2007: Evolution of angular momentum in the 2 June 1995, Dimmitt, Texas tornado. *J. Atmos. Sci.*, **64**, 1365-1378.

—, —, R. P. Davies-Jones, C. A. Doswell III, F. H. Carr, M. D. Eilts, and D. R. MacGorman, 1994: Verification of the Origins of Rotation in Tornadoes EXperiment: VORTEX. *Bull. Amer. Meteor. Soc.*, **75**, 995-1006.

—, —, M. S. Gilmore, and R. P. Davies-Jones, 2006: A preliminary survey of rear-flank descending reflectivity cores in supercell storms. *Wea. Forecasting*, **21**, 923-938.

Ray, P. S., B. C. Johnson, K. W. Johnson, J. S. Bradberry, J. J. Stephens, K. K. Wagner, R. B. Wilhelmson, and J. B. Klemp, 1981: The morphology of several tornadic storms on 20 May 1977. *J. Atmos. Sci.*, **38**, 1643-1663.

Shapiro, A., and K. M. Kanak, 2002: Vortex formation in ellipsoidal thermal bubbles. *J. Atmos. Sci.*, **59**, 2253-2269.

Straka, J. M., and J. R. Anderson, 1993: The numerical simulations of microburst-producing thunderstorms: Some results from storms observed during the COHMEX experiment. *J. Atmos. Sci.*, **50**, 1329-1348.

—, and T. R. Mansell, 2005: A bulk microphysics parameterization with multiple ice precipitating categories. *J. Appl. Meteor.*, **44**, 445-466.

Wakimoto, R. M., and H. Cai, 2000: Analysis of a nontornadic storm during VORTEX 95. *Mon. Wea. Rev.*, **128**, 565-592.

—, C. Liu, and H. Cai, 1998: The Garden City, Kansas, storm during VORTEX 95. Part I: Overview of the storm's life cycle and mesocyclogenesis. *Mon. Wea. Rev.*, **126**, 372-392.

—, H. V. Murphrey, and H. Cai, 2004: The San Angelo, Texas, supercell of 31 May 1995: Visual observations and tornadogenesis. *Mon. Wea. Rev.*, **132**, 1269-1293.

Walko, R. L., 1993: Tornado spin-up beneath a convective cell: Required basic structure of the nearfield boundary layer winds. *The Tornado: Its Structure, Dynamics, Prediction, and Hazards*, Amer. Geophys. Union, 89-95.

Weisman, M. L., and J. B. Klemp, 1982: The dependence of numerically simulated convective storms on vertical wind shear and buoyancy. *Mon. Wea. Rev.*, **110**, 504-520.

—, and C. A. Davis, 1998: Mechanisms for the generation of mesoscale vortices within quasi-linear convective systems. *J. Atmos. Sci.*, **55**, 2603-2622.

Wurman, J., J. M. Straka, and E. N. Rasmussen, 1997: Design and deployment of a portable, pencil-beam, pulsed Doppler radar. *J. Atmos. Oceanic Technol.*, **14**, 1502-1512.

Ziegler, C., E. N. Rasmussen, T. R. Shepherd, A. I. Watson, and J. M. Straka, 2001: The evolution of low-level rotation in the 29 May 1994 Newcastle-Graham, Texas, storm complex during VORTEX. *Mon. Wea. Rev.*, **129**, 1339-1368.

REVIEWER COMMENTS

Editor's Notes: Reviewer A joined the authorship roster after his initial (first-round) review. His substantive comments resulted in sufficient upgrade to the manuscript prior to his co-authorship to warrant inclusion herein; and numerous minor comments and wording suggestions (not shown) also were incorporated. Reviewer B performed review only for the initial submission. Reviewer C performed review of both initial and second review drafts. Salient/substantive portions of all three reviews are reproduced herein.

[Authors' responses in *blue italics*.]

REVIEWER A (Robert P. Davies-Jones):

Initial Review:

Recommendation: Accept with Major Revisions

General Comments: The observations of vortex arches connecting counter-rotating vortices in the rear flank of supercells is interesting because it is relevant to tornadogenesis in at least some cases observed during VORTEX and elsewhere. The authors fail to point out that their mechanism has been proposed before. I regret that this review is egocentric because much of the unacknowledged prior work is my own.

This previous work has now been acknowledged.

Substantive comments:

1. There is some confusion concerning whether the vortices are on the gust front or behind it. In the introduction, it is stated that there is a cyclonic vorticity center (or more simply a cyclonic vortex) and a gust front extending from this vorticity center (vortex) into an anticyclonic vorticity center (vortex). Later, in Section 4c, it is said that "the gust front had surged roughly 10 km ahead of the developing (Dimmitt) tornado" and that "the vortices (in the idealized simulation) lag well behind the surging low-level gust front". This inconsistency needs to be eliminated by modifying the sentence in the introduction.

This has been addressed. As in the Dimmitt case the gust front surges eastward and southward from the cyclonic member of the vorticity couplet and the turns back westward to the anticyclonic couplet. This is what happened in the Dimmitt case. And this is what occurs in the simulations.

2. Additional prior work needs to be acknowledged. [Weisman and Davis (1998) and Shapiro and Kanak (2002) are mentioned in the conclusions.] The idealized simulation really is a demonstration of ideas put forward by Davies-Jones et al. (2001 *Meteor. Monogr.*, No. 50., pp 181-186) and references cited therein (Davies-Jones 1996a, 2000a). The encyclopedia article, Robert Davies-Jones, "Tornado", in AccessScience@McGraw-Hill, <http://www.accessscience.com>, DOI 10.1036/1097-8542.701400, last modified: July 21, 2000, describes the vortex-formation mechanism from the generation of vortex rings in the downdraft and the subsequent tilting of these rings as their leading edges move downstream and enter the updraft.

The work of Davies-Jones has now been cited. We were unaware of any other relevant citations.

3. With regard to [former] footnote 3 and its associated sentence in Section 4d, the authors should read the paper by Davies-Jones (2006 JAS p. 658) and references cited therein. Based on his own work and previous work by others, Davies-Jones describes exactly how vortex lines evolve in a baroclinic fluid.

The footnote has been removed.

4. It should be mentioned in Section 4b that, although shear is not explicitly included in the simulation, the location of the downdraft at the rear of the updraft is an implicit effect of shear. Without shear, the rain would be distributed symmetrically relative to the updraft axis.

We have included this in the text.

5. Given that there is little cold air detected at the ground beneath the Dimmitt storm and near several other strong tornadoes observed during VORTEX (Markowski et al. 2002), it seems doubtful that a purely baroclinic process is sufficient to explain tornadogenesis in these cases (as admitted in the abstract and conclusions). A barotropic mechanism such as the one proposed by Fujita (see Preprints of the 1973, 1975 Severe Local Storms Conferences) and simulated by Davies-Jones (see Preprints of the 2000, 2006 Severe Local Storms Conferences) may be far more significant.

These have been cited (Davies-Jones).

6. Advection only advects vorticity around, as in a barotropic forecast model. It does not shrink tubes. The vortex-stretching term in the vector vorticity equation stretches vortex tubes. Vorticity only increases if vortex tubes are stretched longitudinally. Presumably, shrink here refers to lateral shrinking and associated longitudinal stretching. However, shrinking customarily refers to longitudinal shrinking, which is associated with decreasing vorticity.

This has been corrected in the new text.

7. [Section 5, first paragraph. It should be pointed out that there is no barotropic vorticity in the simulation at $t = 0$ because there is no wind at this time. Thus, all the baroclinic vorticity is generated as rings around either the bubble or positive buoyancy anomaly (after $t = 0$) or around the center of negative buoyancy. Can we prove that the arches form from the vortex lines around the negative buoyancy center?]

[Addressed by new author set in revisions.]

[*Minor comments omitted...*]

REVIEWER B (Charles A. Doswell III):

Initial Review:

Recommendation: Reject/revise

General Comments: My general impression of this paper is that it contains a LOT of hypothesizing, some ranting, and a distinct lack of compelling EVIDENCE. My recommendation is that it be rejected in its present form. However, at the same time, I believe that the authors are pursuing a potentially useful line of thought that I do NOT dismiss out of hand. They could very well be on to something very important.

But this paper falls somewhere in a kind of no-man's land. In the absence of hard evidence, I'd say it could be shortened into a brief note focused mainly on the idealized numerical simulation. On the other hand, a convincing demonstration of the validity of their hypothesis would probably depend on another field program to provide the necessary data.

Given the current moribund state of VORTEX II, I probably would feel a LOT better about a shortened version, hopefully with better illustrations and less ranting about their battle with "traditional thinking" - that was primarily about the simple model simulations they've run. I'm NOT disputing the potential value of their hypothesis, but a whole paper about a hypothesis based on a simplified numerical simulation is just not reasonable to me.

Ideas are dime a dozen, and lots of people have ideas - some good, mostly bad. Substantial validations of those ideas are much harder to come by, but offer much more meaningful publications.

1. General comment (a) to Conzemius/Doswell: We have verified the bulk explanation in the simplest way we know how for what is observed. A more complete dynamical explanation probably would best be given in subsequent paper(s). We are only posing a hypothesis here and showing that it is a plausible fluid dynamics evolution. To dig deeply into the dynamics might imply we are trying to prove something that really ought to be considered to be preliminary.

2. General comment (b) to Conzemius/Doswell: We have removed the philosophical means of obtaining a numerical solution for complex fluid dynamic solutions. We do believe in using simple models to explore complex concepts to best try to understand them. Doswell seemed to think, it seems, that we were putting down simple models. On the contrary we are advocating them in the early stages of research.

Walko's paper does not use the word "sag" or "depressed" at all, and it's pretty unclear to me just how the proposed pattern obviates what I interpret Walko to be saying. If this is a strawman to be knocked down, then I think it deserves a much more extensive description that is clearly and obviously related to what Walko was saying in his paper. This doesn't accomplish that.

This is a strawman and is described in much more detail later in the paper. If one draws the Walko scenario you get depressed vortex lines. The word depressed come from our usage. Walko did not look at this possibility or[this] part of the problem.

Forgive me, but it seems to me that having a downdraft trailing a gust front, with intense ascent along the gust front and a gradient of vertical motion (gradients point toward larger values, so wouldn't it be forward-directed?) is not some new revelation. This has been around at least since Lemon and Doswell (1979). With an axis of strong winds blowing from rear to front at low levels, there is naturally a region of cyclonic vertical vorticity to the left of that flow and anticyclonic vertical vorticity to its right. I guess I just don't see this as some revelation, but perhaps I'm missing something?

Perhaps this criticism was written before Dr. Doswell had contemplated the entire article. Dr. Doswell is correct that the gradient is forward-directed in the region of interest. And it is certainly correct that if there as an axis of strong winds, there must be cyclonic vertical vorticity to the left and anticyclonic to the right (unless flow curvature negates the effect of shear). Indeed, as he knows, vorticity is simply a spatial derivative of velocity, and obviously this is not a revelation. What Dr. Doswell missed is that our work ties all of these kinematic features together using the simple description "vortex line arches", and then the paper proceeds to develop a hypothesis for the development of the arches. Hence, the hypothesis explains the evolution of the entire low-level rear-flank flow structure. This sort of explanation was not proffered in Lemon and Doswell (1979), nor in the observational studies that paper summarized.

[Minor comments omitted...]

REVIEWER C (Robert Conzemius):

Initial Review:

Recommendation: Accept with Major Revision

General/substantive comments -- The paper presents the vortex arching mechanism as a hypothesis for the generation of vertical vorticity couplets on either side of the rear flank downdraft, rearward of its gust front. The authors first present a number of observational cases that demonstrate the existence of the counter-rotating vortices and then address the problem by performing an idealized numerical simulation of a downdraft/updraft couplet in shear-free conditions and analyze the kinematic structure of the developing flow. They conclude that the vortex arching process is a plausible mechanism for the development of the vortex couplets (although not the only one possible).

I find the study is worthy of publication in the EJSSM. It constitutes original research in the field, and the authors have presented the evidence to show that the vortex arching process is capable of producing counter-rotating vortices that commonly have been observed in association with tornadic and non-tornadic supercell thunderstorms. The authors apparently see a need to justify a relatively simplified, idealized numerical simulation as a valid approach. However, I do not see this need because I agree with the use of simplified simulations to gain insight into the mechanisms at work in vortex genesis and other fluid processes. To the contrary, one could also argue that similar kinematic analyses could be done on high-resolution simulations that have already been conducted (provided the data have been saved), but I think the simple approach could do just as well.

I think the kinematic analysis of the idealized simulations presented in section 4c is reasonably solid. However, I would like to have seen more quantitative analysis in section 4d. The discussion in that section begins with ruling out certain types of analyses because they are too complex. I think that discussion can be avoided if one technique is chosen and the data are presented. The presentation of quantitative information could come in either (or both) of two forms:

- 1) Present a table showing the terms in the vorticity budget for the three points you analyzed in the section. I think this should be done at a minimum.
- 2) I think the section might benefit from an analysis like that done in some papers on mesoscale convective vortices. That analysis would be to use the vorticity equation in flux form. In particular, the technique is based on Haynes and McIntyre (1987). See JAS Volume 44, Issue 5. Chris Davis at NCAR has also applied that analysis in some of his MCV papers, which include Weisman and Davis (1998), and Davis and Trier (2002). The advantage of using the vorticity equation in flux form is that the area average vorticity can be calculated using line integrals around the area of choice. A possible disadvantage is that the terms would have to be interpreted slightly differently because they are formed from combination of terms in the advective form of the vorticity equation.

[Minor comments omitted...]

General Reply [also see “General comments to Conzemius/Doswell” above]:

Thank you for your carefully thought-out review. It has made for a much better paper.

Second review:

I'm not sure the authors read all of my previous suggestions or found them useful. It looks like the vorticity budget terms have been calculated, although the method I suggested (flux form) was not used. In the flux form of the vorticity equation, the tilting term no longer appears as a separate term and is therefore difficult to interpret. Because tilting is an important mechanism for vertical vorticity generation in the idealized simulation presented in this paper, the flux form of the vorticity equation may have somewhat limited usefulness for this analysis.

It might be interesting to see what the results would be to perform a sensitivity experiment with different amounts of rain (in addition to the shear experiments, which are already planned), but that would be a topic for future study. It might be one way to further explore the role of the descending reflectivity core. The addition of Figure 5 was helpful in understanding the proposed mechanism.

We performed simulations with different rain rates and with different size rain areas. Though there were quantitative changes, the qualitative changes were nil. We therefore chose the most representative case for the paper. Thanks for asking about different rain rates.

[Minor comments omitted...]